

Master Thesis

CODEN:LUTMDN/(TMMV-5272)/1-45/2016



LUND UNIVERSITY
Lund Institute of Technology



**Machinability analysis of cemented carbide
-A theoretical and experimental study**

Oskar Sörén

2016

DEPARTMENT OF MECHANICAL ENGINEERING
LUND INSTITUTE OF TECHNOLOGY

Preface

This master's thesis has been accomplished at Sandvik Coromant in Gimo, with guidance from the department of Production and Materials Engineering at the Faculty of Engineering, LTH at Lund University. The thesis was completed between September 2015 and January 2016.

First off I would like to express my appreciation to my supervisors at Sandvik Coromant, Per Melin and Jan Willem Mollema for all their help and guidance. I also want to thank all the people at Sandvik Coromant that in any way helped me during my time at the company.

I also want to express my gratitude to my supervisor docent Volodymyr Bushlya at Lund University (LTH) and also my Examiner, professor Jan-Eric Ståhl for helping me in various matters during the project.

Lund, January 2016

Oskar Sörén

Abstract

Sandvik Coromant is the market leader of producing tools for advanced metal cutting. The tools are produced in cemented carbide, however Sandvik Coromant does not produce tools for machining cemented carbide. The aim of the thesis was to perform cutting tests in cemented carbide with diamond tools to investigate if the binder content affected the machinability of the process.

The wear tests were performed in cemented carbide with two different binder contents H10F and H15F. H10F consist of 10% cobalt and 90% tungsten carbide while H15F consist of 15% cobalt, 84.3% tungsten carbide and 0.7% other. Two different types of tools were used in the experiment, a diamond coated cemented carbide ball nose mill and a nano-polycrystalline diamond ball nose mill.

The wear tests were performed in a 5-axis mill from Mikron HSM200uLP and the tool wear was measured in an optical 3D microscope from Alicona. The surface of the workpiece was examined using a scanning electron microscope (SEM) and the surface roughness using a 3D optical microscope from Veeco in Västberga.

The results show that the machinability is not affected by a change in binder content from 10 to 15% cobalt. Tool life and surface quality are more dependent on tool shape and tool material. The surface roughness obtained in the experiments range from 0.12 μm to 0.38 μm in R_a . Since the experiment did not focus on obtaining the optimal surface roughness it could be possible to select different cutting data in order to optimize the surface roughness.

Future work could include testing of other tool materials such as nbcBN.

Table of contents

1	Introduction	4
1.1	Background	4
1.2	Definitions and nomenclature	5
1.3	Background to the project and project definition	5
1.4	Method	6
2	Theoretical framework	8
2.1	An introduction to cutting	8
2.2	Workpiece material	10
2.3	Tool material	13
2.4	Machinability	15
2.5	Conclusion	22
3	Experiment	23
3.1	Experimental setup	23
3.2	Expectations	28
3.3	Experimental results and discussion	29
4	Conclusions	41
5	Future work	42
	<i>References</i>	43

1 Introduction

1.1 Background

1.1.1 Company

Sandvik Coromant is the ‘market-leader for tools and tooling systems for advanced industrial metal cutting. Products are manufactured in cemented carbide and other hard materials such as diamond, cubic boron nitride and special ceramics’ [1]. Sandvik Coromant is a part of Sandvik Machining Solutions, which is a part of Sandvik Group. Sandvik Coromant has 8 000 employees and is represented in 130 countries [2].

Sandvik was founded in 1862 and was originally a steel manufacturing company, but has over the years developed to include many different branches. ‘Our heritage is steel but the real history of Sandvik Coromant started in 1942 when Wilhelm Haglund was assigned the job as manager for a new production unit for cemented carbide tools in Sandviken, Sweden’ [3]. The headquarter of Sandvik Coromant is located in Sandviken, Sweden. Sandvik Coromant’s largest production unit for cemented carbide is located in Gimo, which is also the base for this master thesis.

1.1.2 Products

Sandvik Coromant produces a broad range of tools, mainly used for milling, turning, drilling, threading, boring and tapping [4]. Milling tools can be divided into two categories based on the design of the tool: solid tools and cutter bodies with replaceable inserts, see Figure 1 and Figure 2.



Figure 1 - Solid mill from Sandvik Coromant [5].



Figure 2 - Ball nose milling cutter with inserts from Sandvik Coromant [6].

Sandvik Coromant categorises the milling tools in terms of their application, such as: face milling, gear milling, high feed milling, parting and grooving, profile milling, round tools milling, chamfer milling, shoulder milling and silent tools [4].

Tool holders with changeable inserts provide the possibility to replace the insert when it is worn out, which can lead to lower tool costs compared to solid tools. The tool holders also provide the option to choose between a broad range of insert geometries to optimise the production. Solid tools are stable and can be produced with very small geometries. They can often be ‘reconditioned after extended use, usually through resharpener or through preparation of the cutting edge in other ways, as well as providing them with wear-resistant coating’ [7] to ensure an economical production.

The choice of tool is not arbitrary and a lot of knowledge goes into choosing the right tool for the job. The focus of the thesis was on solid tools.

1.2 Definitions and nomenclature

Following is a list of standardized words and expressions that are used in the report.

- The abbreviation nbcBN is used instead of the term nano-binderless cubic boron nitride.
- NPDB is a nano-polycrystalline diamond ball nose tool from Sumitomo.
- When speaking of cemented carbide the sintered state of the material is being referred to.

1.3 Background and project definition

Sandvik Coromant is the market leader of producing tools for milling, turning and drilling, used for machining metals and composites. However Sandvik Coromant does not manufacture tools for machining cemented carbides, which is Sandvik Coromant's primary tooling material.

In today's ever changing market it is crucial to lead the development of new products and be on top of technology. Therefore it is Sandvik Coromant's aim with this project to study the effect of binder content in cemented carbide when machining with diamond tools. This information will help future applications in machining cemented carbides.

Cemented carbide is a type of composite material, where two or more materials are combined in order to create a new material with improved characteristics. The aim is to combine one or more hard, but brittle carbides with a tough binder metal so that the outcome is both hard and tough.

‘All cemented carbides have tungsten carbide (WC) as their most important hard phase, but they often contain either carbides, carbonitrides or nitrides of titanium, niobium, vanadium or chromium as well’ [7]. As binder cobalt is most common, but both nickel and iron are used as well. The material characteristics of cemented carbide can be designed for the application it is used for by choosing the input content. Also the amount of binder versus carbide influences the material characteristics and can be altered depending on what characteristics are desired. This binder/carbide ratio is thought to influence the machinability of the material in terms of product quality, tool wear and process stability.

The purpose of the project was to investigate and analyse the possibilities regarding milling in cemented carbides, both theoretically and experimentally. The focus was to study how the binder content in cemented carbides affected the machinability, and also study what effect choice of tool material had on the process.

This background lead to the following main question:

How is the machinability of cemented carbide affected by the binder content in terms of tool life, surface quality and an economical aspect, when machined with coated cemented carbide or diamond tools?

The main question can be divided into sub questions, to better help answering the main question:

- *What is the definition of machinability?*
- *How can cemented carbide be machined in an efficient way?*
- *What surface quality can be obtained, and how can this be measured?*
- *What is surface integrity and what does the machined cemented carbide surface consist of, after machining?*
- *Should the milling process include cooling for an optimal process, and if so what kind of cooling medium?*
- *Is there an economically preferable binder content?*

1.4 Method

In order to answer the questions, a literature survey was conducted to gather theoretical background regarding cutting of cemented carbide. Research of wear behaviour and wear mechanisms of cemented carbide as a tool material has been thoroughly researched during the past decades. However not much research of material removal characteristics of cemented carbides as a work material, cut by hard tools, has been done. [8]

Because the tool material needs to be harder than the work material during a cutting process the choice of tool material is limited. Focus was on diamond as tool

material, because of its hardness that suits the experiment. One coated cemented carbide tool was also tested. The tool is predicted to have a shorter life span but is a cheaper option. Since cutting of cemented carbide with diamond tools are a fairly unresearched subject, experiments were conducted in order to further answer the questions at hand.

Equipment to analyse the cut surface, tools and chips was made available at Sandvik Coromant plant located in Gimo and also at a research and development office in Västberga. The equipment will be presented later on in the paper.

2 Theoretical framework

In this chapter information from the literature survey is presented in order to answer some of the questions from the previous chapter. The questions that will be answered are:

- *What is the definition of machinability?*
- *How can cemented carbide be machined in an efficient way?*
- *Should the milling process include cooling for an optimal process, and if so, what kind of cooling medium?*
- *What is surface integrity?*

The chapter will also explain how surface roughness can be measured.

2.1 An introduction to cutting

During a cutting process, workpiece material is removed with use of a cutting edge. This can be illustrated by a knife cutting butter, it is clear that the cutting edge has to be harder than the workpiece material for a successful cut. Also the internal stability of the workpiece influences the outcome of the cutting operation. If the stability is high enough, material will leave the workpiece in form of chips, otherwise deformation of the workpiece will occur and result in burr formation or fractures [7]. This suboptimal cutting may lead to scrapping of the workpiece or additional steps of machining, which will increase the machining cost. An illustration is presented in Figure 3.

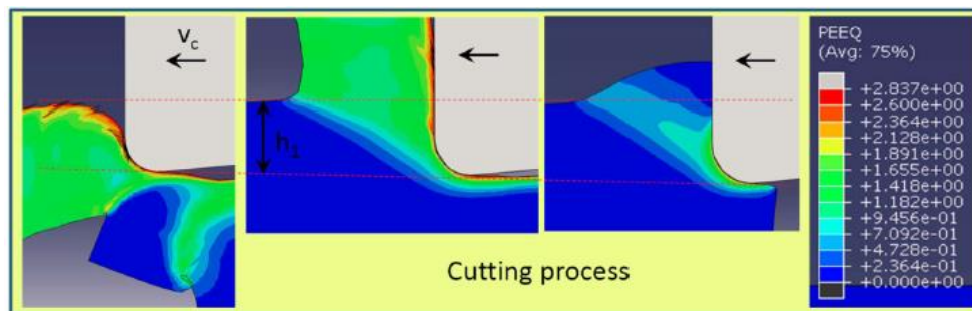


Figure 3 - Illustration of a cutting process [7].

Two types of cutting processes can be distinguished, continuous and intermittent cutting. Intermittent cutting is characterized by a cutting edge being engaged and disengaged in intervals while in continuous cutting the cutting edge is engaged during the whole period of time the cutting takes place [7]. Turning is an example of continuous cutting and milling is a typical intermittent process. The different processes demand different characteristics of the tool material. Continuous cutting

‘places stronger demands on wear resistance and heat retention level of the cutting tool’ and an ‘intermittent process place stronger demands on the cutting tool’s toughness and flexural strength’ [7].

The cutting process is determined by cutting data and the data can be altered in order to optimize the process. A lot of knowledge is needed to optimize a cutting process and the tool manufacturer often provide general information regarding cutting data for different conditions. A couple of cutting data parameters are presented below:

Spindle speed (n) represents to what speed the spindle revolve and is measured in Revolutions Per Minute (RPM).

Cutting speed (v_c) is measured as the relative speed of movement between the tool and the surface of the workpiece, regardless if one of them stands still or both move. Cutting speed is usually measured in m/min and calculated as:

$$v_c = \frac{2\pi * R * n}{1000} \quad (1)$$

Where R is the cutting tool radius (m).

Feed rate (f) is the axial or radial movement of the tool or workpiece that takes place during a revolution for one or the other. Feed rate is normally measured in mm/min. The feed can also be presented as feed per tooth for multi-edge cutting processes. The total feed is then presented as the sum of the active tool edges.

Cutting depth (a_p) describes the depth of cut perpendicular to the feed and is specified in mm.

Cutting width (a_e) describes the depth of cut parallel to the feed and is also specified in mm. [7]

As the milling machines, tools and processes evolve, the bar of what is possible to machine is raised. In the recent years the market for mini products has increased rapidly. A couple of markets that demand smaller and smaller products are consumer electronics, medical and dental. To meet the demand of these markets conventional milling has advanced to what is called micro-milling. Generally micro-milling is used to produce small parts or parts with a fine surface roughness.

A couple of requirements need to be met if a micro-milling operation is going to be successful. To begin with the machine that is used need to be rigid in order to avoid vibrations. The guideway system needs to be accurate and free from disturbing friction and glitches. The same requirement applies to the drive and motion technology of the machine. The spindle speed is of importance when micro-milling, and a smaller tool diameter requires a higher spindle speed. This is

explained by the cutting speed equation (1). It can be seen that if the tool diameter decreases the spindle speed needs to increase in order to keep the cutting speed constant. ‘With micro-milling, tool size is relative to the application. Commonly, a 6-mm-diameter tool would be considered large and a 0.3-mm-diameter tool would be considered quite small. In this range, a spindle speed of 50 000 RPM would provide an adequate solution’ [9]. Researchers expect to reach spindle speeds up to 1 000 000 RPM [10], but spindles of today more likely operate with a maximum of 45 000 RPM [11].

During the cutting process heat is developed in the tool and workpiece. To lower the cutting temperature cutting fluid can be used. Cutting fluid can be water based emulsions, oil or gas. The different types of cutting fluids have varying characteristics and are used in various applications. Emulsions has great cooling effects due to its high water content (up to 99%) [12] and are used to lower the process temperature. Oil based cutting fluids are mostly mineral oils with additives to improve friction and are mostly used in operations that require lubrication.

When micro milling cemented carbide, cutting fluid is preferably used to remove chips from the cutting edge to prevent them damaging the workpiece surface. Cutting fluid can be applied in different ways, for example by wet cooling, mist cooling or high pressure cooling. Most cutting fluids are environmentally unfriendly but there are environmentally friendly cutting fluids, such as vegetable-based cutting fluids. Also techniques to apply small quantities of fluids are available such as minimum quantity lubrication (MQL) [13].

In many cases cutting fluid is not necessary for the cutting process. The choice between dry machining or to use a cutting fluid should balance the effect of the shorter tool life due to higher cutting temperature and the positive environmental effect of not using a cutting fluid. It is not arbitrary to choose the right cutting fluid and fluid distribution. Both are highly dependent on the type of workpiece material, tool material and how tough the machining process is. Often the tool manufacturer provides information to ease the selection.

2.2 Workpiece material

Two types of cemented carbide are selected as workpiece material: H10F and H15F. The numerical parts refer to the binder content. The ‘F’ refers to the grain size which is of importance because the size affects the material characteristics of the material. A finer grain size means a higher hardness for a given binder [14]. The grain size range from nano ($< 0.2 \mu\text{m}$) up to coarse ($> 2.0 \mu\text{m}$) [15]. Both of the selected materials have submicron grains (0.5-0.9 μm) of tungsten carbide and a binder of cobalt. H10F consist of 10% cobalt and 90% tungsten carbide while H15F consist of 15% cobalt, 84.3% tungsten carbide and 0.7% other materials [16] [17].

2.2.1 Manufacturing of a cemented carbide insert

Cemented carbide is a metal powder metallurgy material that is manufactured in several steps. At first ingredients such as tungsten carbide, cobalt and other chemicals are weighed and crushed to a powder in a grinder and mixed. Often wet grinding is used when producing the powder, and the mixture is then spray dried to remove the liquid. The grain size is controlled by the grinding time, a longer grinding time result in finer grains.

When the powder is dry it is pressed in a mould using a die and two plunges, to get the right shape. The pressing results in what is called a green body that has a geometry as close as possible to the finished product. The green body has low strength and is highly porous. After pressing a sintering process is needed to create the properties of cemented carbide. During the sintering process the green body is exposed to temperatures ranging from room temperature up to about 1400 °C, in several steps. In the sintering process tungsten particles are fused together and the cobalt is melted and binds the tungsten carbide particles together. The sintering results in shrinkage of 45% of the volume [7].

After sintering the tool is ground to meet geometrical tolerances. The tool can also be edge treated to round off the edge, which results in a stronger edge. As a last stage the tool can be surface treated with different coatings to improve its wear resistance. The surface treatment involves either Chemical Vapour Deposition (CVD) or Physical Vapour Deposition (PVD). The coatings can be of different thickness and the number of layers can be altered, in order to obtain the wanted characteristics. A schematic overview of the cemented carbide process is presented in Figure 4.

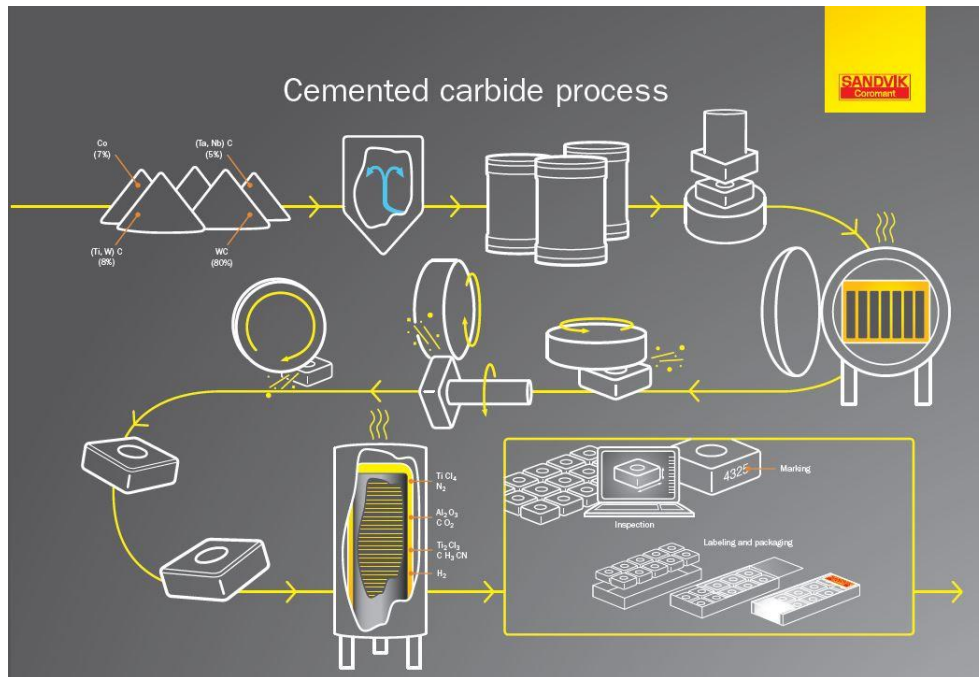


Figure 4 - Cemented carbide process.

2.2.2 Material characteristics of cemented carbide

Thanks to the combination of hardness and toughness, cemented carbide constitutes a reliable option as tool material for inserts and solid tools. The tool material is well researched and has been used a long time. The first cemented carbide tool was presented at the Leipzig Trade Fair in 1926, by the German corporation Krupp [7]. The material characteristics can be altered to fit the application at hand by selecting different input materials, grain sizes and composition. Therefore the material can be made very tough to fit intermittent cutting for example. The material properties of the selected cemented carbides can be seen in Table 1 [16] [17].

Table 1- Material data for H10F and H15F.

Grade	Hardness		Compressive strength MPa	Density g/cm ³	Corrosion resistance 0-10	Wear resistance 0-10
	HV30	HRA				
H10F	1600	92,1	6 250	14,45	4	5
H15F	1400	90,4	5 300	13,95	4	6

Corrosion and wear resistance data is subject in accordance with 0 = very low and 10 = very high resistance.

2.3 Tool material

Not many tool materials are suitable for milling cemented carbide and ‘conventional tools are insufficient in chipping resistance, wear resistance and edge sharpness’ [18]. Research to improve tool materials for cutting cemented carbide is constantly raising the bar of what is possible. For this experiment the selected tools were:

- A diamond coated cemented carbide ball nose end mill from Zecha called 900.0300.150.060, illustrated in Figure 5.
- A binderless nano-polycrystalline diamond tool from tool manufacturer Sumitomo called NPDB 1050-20, illustrated in Figure 6.

The NPDB tool is part of the newest tool material technology, the tool was commercially released as build-to-order in April 2013 and in stock from October 2014 [19].



Figure 5 - Diamond coated cemented carbide ball nose end mill from Zecha [20].

Figure 6 – Binderless nano-polycrystalline diamond ball nose end mill from Sumitomo [21].

2.3.1 Manufacturing and material characteristics

2.3.1.1 NPDB

Diamond is the hardest known material in the world, and can be manufactured by sintering of selected diamond particles at high pressure and temperature. There are different types of diamonds with different hardness. Either the diamond has a monocrystalline structure or a polycrystalline structure. Much like cemented carbide, the polycrystalline diamond contains diamond grains that are sintered with a metallic binder [22]. The monocrystalline structure is common in gemstones and is both naturally occurring and manufactured synthetically. A diamond is composed by carbon atoms that are arranged in cubic networks, the structure provides the hardness of the diamond. Allotropes of diamonds are graphite,

amorphous carbon and buckminsterfullerene. What is in common for the materials are that they all are carbon based materials.

The researchers at Sumitomo have created a binderless diamond with grains in the nanometre scale, called nano-polycrystalline diamond (NPD). The edge sharpness of a tool is dependent on the grain size and a finer grain leads to a possible sharper edge. This single-phase diamond is created ‘by directly converting graphite into diamond, allowing particles to be bound together under ultrahigh-pressure and high-temperature conditions (15 GPa or higher and 2200 °C or higher)’ [18].

The diamond can then be shaped to the desired geometry. Traditionally diamonds are machined with grinding operations, though grinding has geometrical restrictions. Electric discharge machining (EDM) can be used to shape the diamond into more complex geometries, if the diamond contains a conductive binder [7]. Since the NPD is binderless, a totally new machining technique was developed by Sumitomo [18], unfortunately no further explanation has been found in the literature survey explaining the technique.

The edge sharpness of the tool is important because it correlates to some extent to the surface roughness it can produce. Generally a sharper edge can cut a smoother surface. To grind a sharp edge on the tool the carbide particles have to be small, the smaller the particles are the sharper the tool can be. Since the particles of a NPD are in the nanometre scale, tools can be made with superior edge sharpness compared with conventional diamond tools. The surface roughness also depends on the cutting radius of the tool and the undeformed chip thickness, which will be further presented in chapter Chip form and chip properties. The NPD is isotropic and therefore free from uneven wear associated with crystallographic orientation, which leads to high precision milling for a long period of time [18]. A hardness comparison of various hard materials can be seen in Figure 7.

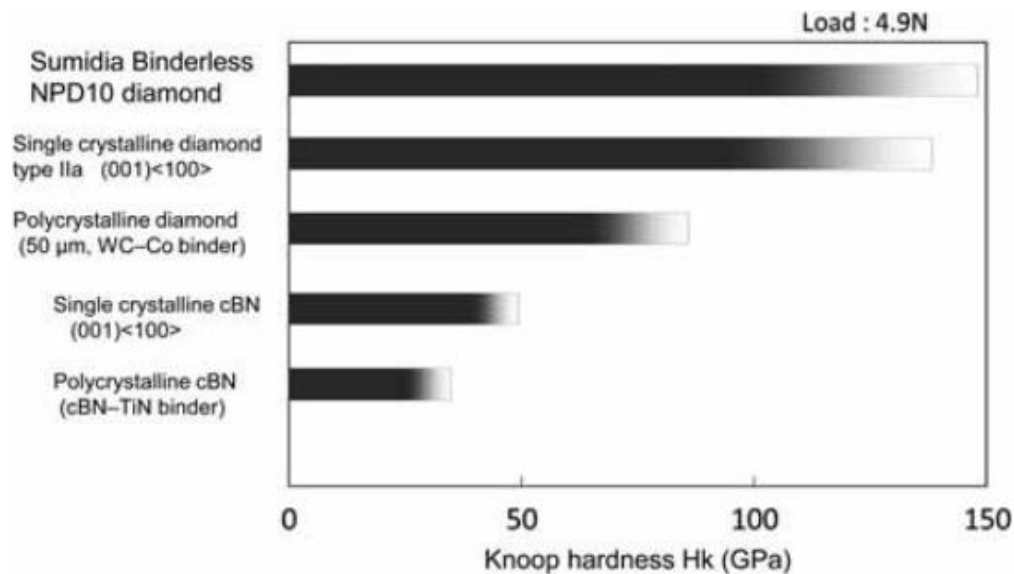


Figure 7 - Hardness comparison among various hard materials [18].

2.3.1.2 Diamond coated cemented carbide

Cemented carbide tools can be used to machine cemented carbide, if the tool has been surface treated with a coating. The cemented carbide manufacturing process is described in chapter 2.2.1. The selected cemented carbide tool from Zecha is provided with a diamond coating to enhance the tool life. The tool life is predicted to be shorter than the NPDB tool, but since the cemented carbide tool is cheaper it might provide a cheaper overall production cost.

2.4 Machinability

Machinability is a complex term, which is built up by numerous factors that contribute to the end result. The machinability is directly linked to the cost of the process and needs to be evaluated in order to obtain an economical production. In the following chapter machinability will be explained and different parts of the term will be presented.

There is no exact definition of machinability. However [7] presents it as:

‘Machinability expresses how readily a particular workpiece material can be machined by a cutting tool in a manner such that certain predetermined levels of form, size and degree of roughness of the surface can be achieved.’

Thus machinability is a way to measure and classify how easily a workpiece can be machined within a certain process. Machinability is a relative term and one process

cannot be compared with another in a standardised way, because of the complexity of relations between the different factors. For example when comparing the machinability of a workpiece material, there are no guaranties that the ranking of materials will be the same for milling as for turning. The main factors can be seen in Figure 8.



Figure 8 - Main factors that influence machinability [7].

Not all categories will be explained further, but a few key ones regarding milling in cemented carbide will be presented.

2.4.1 Wear

To begin with cemented carbide is extremely hard and tough, which was stated earlier. This leads to requirements on the tool material. During the cutting process the tool is subjected to wear. A couple of types of wear can be distinguished:

Flank wear is an abrasive wear and occurs alongside to the cutting speed direction and decreases the clearance angle by continuous wear. Because the clearance angle decreases, the contact length increases between the workpiece and the clearance face. This will cause an increase in contact forces and tribological forces, and an increasing temperature of the process. The increasing forces and temperature can lead to deformation of the workpiece, tool or tool holder.

Crater wear is also an abrasive wear and depends on the types of chips that are produced and takes place on the rake face of the tool. The wear increases the contact length between the rake face and the chips, thus increasing the shearing forces. Crater wear changes the tool geometry, resulting in a weakening of the cutting edge.

Notch wear is a chemical wear and usually occur at the clearance face of the tool. Areas that have been heated to high temperatures react with oxygen in the air and are oxidized. The affected parts can then be easily worn off. Machining work hardened material can also lead to notch wear.

Wear is a complex phenomenon and can be a combination of the different types or occur by itself. Other than abrasive wear there are adhesive wear when workpiece material are welded onto the tool and then chipped away. Diffusion wear happens when atoms diffuse between the tool and workpiece, which change the material characteristics of the affected zones [7]. The important part of wear is that it should be predictable, as with flank wear. If the wear is not predictable total failure can occur at any time and destroy the workpiece and tool, which leads to high production costs and low machinability. The three basic wear types are illustrated in Figure 9 - Figure 11.



Figure 9 – Flank wear [7].



Figure 10 – Crater wear [7].

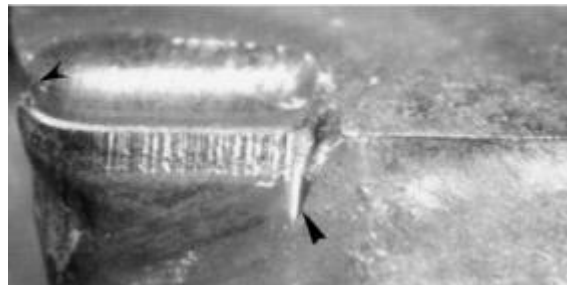


Figure 11 – Local flank wear, so called notch wear on the main and minor cutting edge [7].

2.4.2 Surface integrity

Tool wear directly affects the surface integrity of the machined part which also is included in the machinability term. Surface integrity is described by surface topology, residual stresses, structure and chemical composition of the workpiece. Surface topology can be measured in numerous ways, a usual way of measurement is mean roughness of the profile R_a . As can be seen in Figure 12 the R_a value is measured as a mean value of all deviations from a straight line within a measurement length. The R_a value is not sensitive to individual deviations, but it also means there is a risk of missing large peaks. [23]

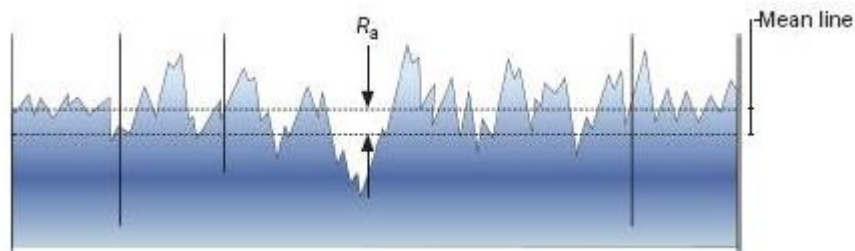


Figure 12 - Example of measurement of mean profile roughness [23].

Another way to measure the surface roughness is the average maximum profile height R_z and is illustrated in Figure 13. The profile height is measured between the highest peak and the lowest valley of each reference length. The average profile height is calculated as a mean value of all the reference profile heights from the measured length. The equation is presented below as equation (2).

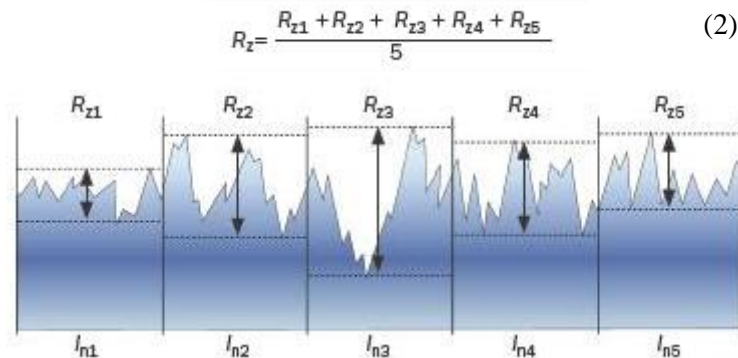


Figure 13 - Average maximum profile height [23].

After a material has been cut there can exist residual stresses in the workpiece. Residual stresses can be either compressive or tensile. A compressive residual stress prevents the occurrence of fatigue. Fatigue is a phenomenon where cracks at the surface of the workpiece are opened and closed by load variations. The crack grows for each cycle in an unpredictable way and eventually breaks. The

compressive residual stress slows down the process by restraining the crack propagation; an illustration can be seen in Figure 14. The tensile residual stress on the other hand, speeds up the process by increasing the crack propagation.

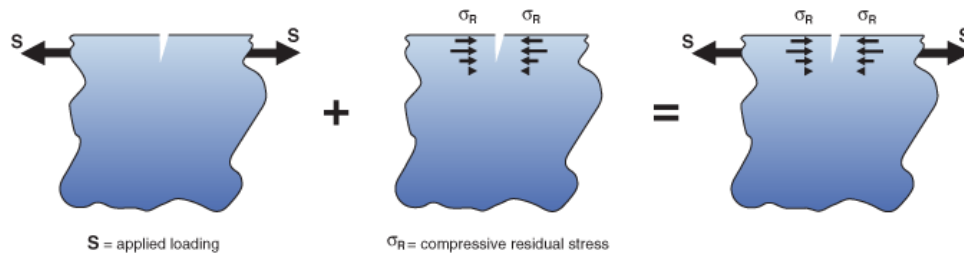


Figure 14 – Compressive residual stress preventing fatigue [24].

The residual stress can be measured using for example X-ray diffraction (XRD).

A SEM is used to determine the chemical composition of the cut surface. During the cutting process heat is generated and the material can undergo phase transformations and oxidation. Also diffusion between the tool and the workpiece can exist.

2.4.3 Chip form and chip properties

There are two types of chip formations: ductile and crack formation. In the case of ductile cutting, the workpiece material is sufficiently tough to be locally deformed by the cutting edge. The deformation leads to a chip being sheared off when the deformation resistance has reached its maximum.

Crack formation appears if the workpiece material behaves in a brittle way. The material is too stiff for deformation or sliding of the material to occur, which leads to cracking. The brittle cracking is an unpredictable process and can damage the surface of the workpiece and the tool. [7]

Cemented carbide is a brittle material and to achieve a low surface roughness the cutting process needs to be ductile. An example of a ductile and a brittle cut can be seen in Figure 15 and Figure 16.

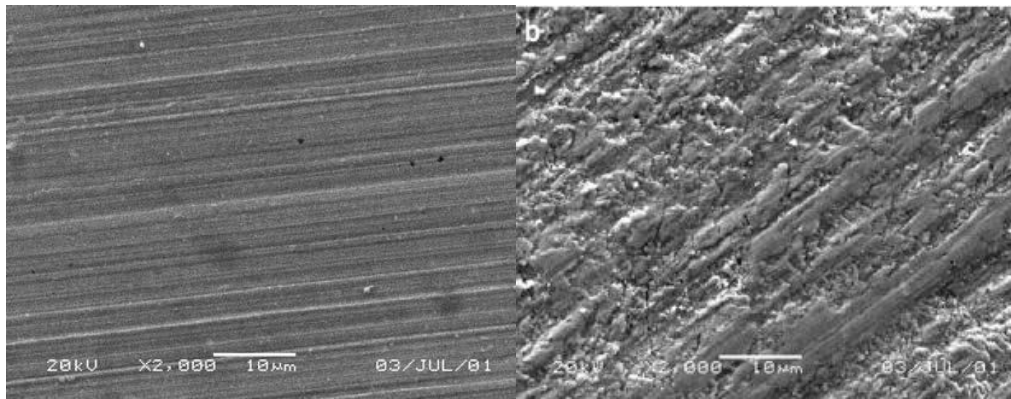


Figure 15 - Ductile cut surface [25].

Figure 16 - Brittle cut surface [25].

There are ways to cut brittle materials in a ductile way. Bridgeman presented in one of his articles that brittle materials can behave in a ductile way, when subjected to high hydrostatic loads [26]. However there is an upper limit to the load, and if brought over the limit the material would crack. The hydrostatic load is dependent on the undeformed chip thickness (a) and the tool edge radius (r) as can be seen in Figure 17. It can be seen that at $a/r < 0.6$ the workpiece material is subjected to great hydrostatic stress. If the hydrostatic load is high enough it suppresses the growth of pre-existing flaws in the workpiece material which prevents brittle shearing.

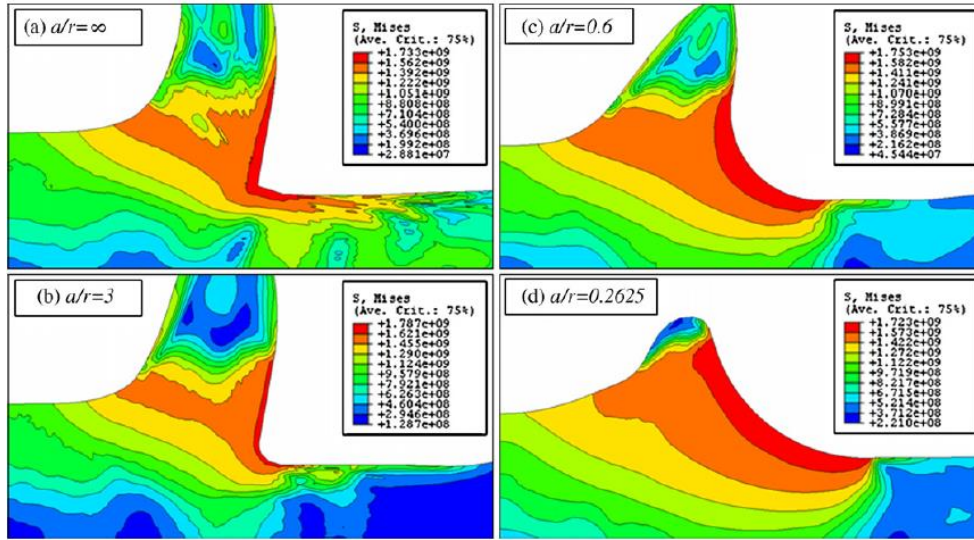


Figure 17 - Stress distribution at (a) $a/r = \infty$, $r = 0$; (b) $a/r = 3$, $r = 1 \mu\text{m}$; (c) $a/r = 0.6$, $r = 5 \mu\text{m}$; (d) $a/r = 0.2625$, $r = 8 \mu\text{m}$ [27].

In [28] Liu and Li presented an energy model for ductile chip formation in cutting of tungsten carbide. It is established that there is a transition between ductile and brittle chip formation that is dependent on the tool geometry, workpiece material and cutting conditions. Experiments show that when the undeformed chip thickness is smaller than a critical value, the chip formation is ductile. The critical value varies for different workpiece materials.

In [25] Liu, Pi and Liang observed that there are two conditions for ductile cutting of a brittle material. The first was to have such a small undeformed chip thickness that the compressive force is large enough to suppress crack propagation. For cemented carbide the critical undeformed chip thickness was theoretically determined to $2,114 \mu\text{m}$ and experimentally to $2,485 \mu\text{m}$. The difference in size was due to a value used in the theoretical model was selected for ceramics instead of cemented carbide. The second condition being the undeformed chip thickness should not be larger than the cutting edge radius. The undeformed chip thickness d_{max} can be calculated as:

$$d_{max} = R - \sqrt{R^2 + f_z^2 - 2f_z \sqrt{2Ra_p - a_p^2}} \quad (3)$$

where R is the tool radius, f_z is feed rate per tooth and a_p depth of cut. To perform a ductile cut the two conditions previously described need to be met. The surface quality obtained by the cutting process is highly dependent on the cutting process being ductile, therefore it is considered a key factor in machinability.

2.5 Conclusion

In the beginning of the chapter three questions were defined and theory to answer them was presented. To sum up the chapter, the questions are answered shortly.

What is the definition of machinability?

There is no definitive definition of machinability, but the general meaning is to describe how readily a workpiece can be machined within a certain process to meet predetermined targets.

How can cemented carbide be machined in an efficient way?

Cemented carbide is a hard and brittle material. To achieve a fine surface the cutting process during milling should be ductile. To mill a brittle material in a ductile way two parameters must be met. The undeformed chip thickness should be lower than a critical value, which is dependent on the workpiece material and has been experimentally determined to be 2,485 μm for cemented carbide. Also the undeformed chip thickness should be smaller than the cutting edge radius of the tool.

Should the milling process include cooling for an optimal process, and if so what kind of cooling medium?

The choice to use a cooling medium or not is a complex issue and is highly dependent on the cutting conditions. Most tool manufacturers provide recommendations for their tools during different cutting processes.

What is surface integrity?

The surface integrity is the term used to evaluate the quality of the surface and/or sub-surface of a component, generated by the machining process. Topography, plastic deformation, hardness, variations in microstructure, residual stress, micro cracking and phase transformation are among the conventional parameters related to surface integrity [29] [30].

3 Experiment

In this chapter the experimental setup is described and the equipment used to analyse the tests are presented. The setup is followed by expectations for the outcome of the experiment. Ending this chapter are results and discussion of the experiments. The experiment was performed in order to answer the following questions:

- *What surface quality can be obtained?*
- *What does the machined cemented carbide surface consist of, after machining?*
- *Is there an economically preferable binder content?*

3.1 Experimental setup

The experimental tests were performed in a 5-axis mill from Mikron HSM200uLP. Workpiece materials selected were H10F and H15F from Sandvik. Tools used as described earlier. The process was cooled using oil mist applied from an external nozzle for the NPDB tools and one coated cemented carbide tool. The remaining tools were dry machined. The milling order can be seen in Table 2 and the cutting data in Table 3.

Table 2 - Experimental setup.

Test number	Tool	Workpiece material	Cooling method
1	Zecha	H10F	Dry machining
2	Zecha	H10F	Dry machining
3	Zecha	H15F	Dry machining
4	Maznada	H15F	Dry machining
5	Sumitomo	H10F	Oil mist
6	Zecha	H15F	Oil mist
7	Sumitomo	H15F	Oil mist

Table 3 - Cutting data.

Cutting data	
Cutting depth (a_p)	0,02 mm
Cutting width (a_e)	0,02 mm
Feed per tooth (f_z)	0,004 mm/tooth
Spindle speed (n)	50000 rpm
Cutting speed (v_c)	40 m/min

Tests were conducted on rectangular pieces of cemented carbide plates with dimensions seen in Figure 18. The manufacturing process of the workpiece was similar to the original tool manufacturing process but no surface coating was applied at the end.

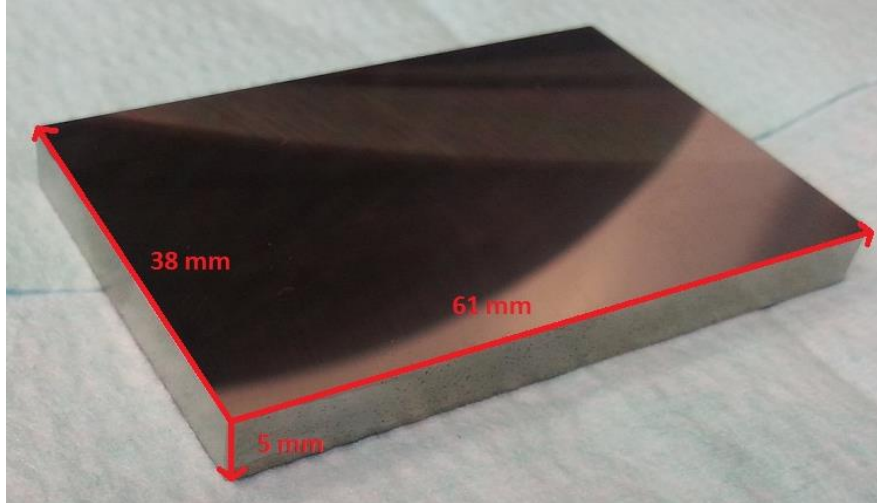


Figure 18 - Workpiece dimensions.

The plates were surface-ground and fitted in a vice in the milling machine. The workpiece was then milled with the specified tools. Tests were interrupted in a predetermined increasing interval of passes. When the tool has travelled one length of the short side of the workpiece, one passing is done. The machine was stopped in the following interval: 2, 4, 8, 16, 32, 64, 128 passes. When the interval had reached 128 passes the remaining area of the workpiece was milled with an interval of 128 passes until the entire workpiece was machined. At every stop in the interval the flank wear (VB) of the tool was measured using an optical 3D microscope from Alicona. An illustration of the cutting path is seen in Figure 19 below.

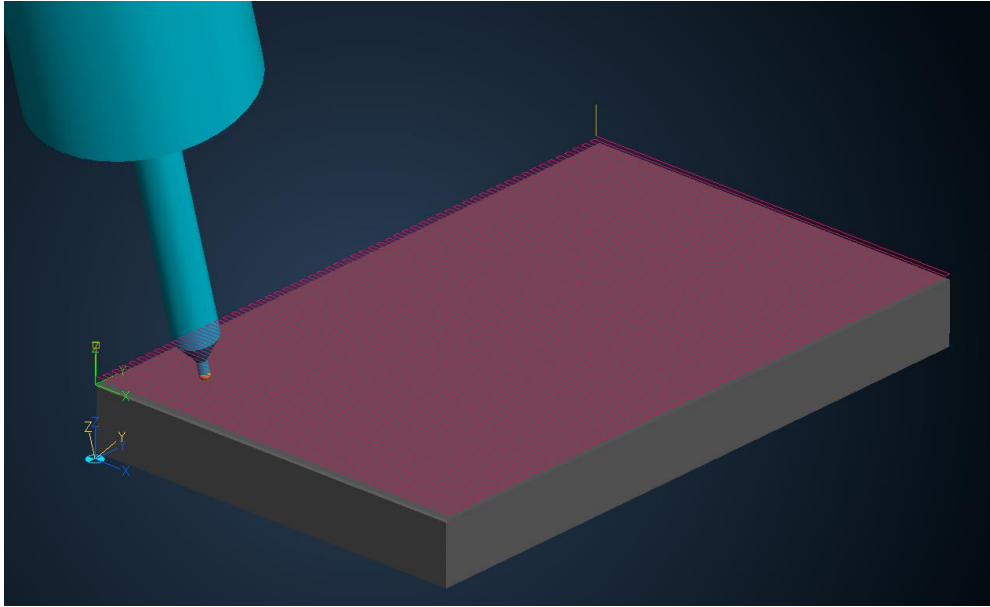


Figure 19 – Cutting path.

The tests were conducted at an angle of 15° and as downward ramping, illustrated in Figure 20. The cutting depth were small, $a_p < a_{p,crit}$ which means that the highest relative speed will occur at R_{ef1} . Since the effective cutting radius changes as the tool is tilted, a new radius is calculated as:

$$R_{ef1} = R * \sin \alpha \quad (4)$$

and the cutting speed as:

$$v_c = \frac{2\pi * R_{ef1} * n}{1000} \quad (5)$$

where v_c is cutting speed (m/min), R is the cutting tool radius (m), R_{ef1} is the effective cutting radius (m), α is the tilt angle of the tool ($^\circ$) and n is the spindle speed (RPM) [31]. When the tool is tilted a larger part of the tool is made available for cutting. When the tool is perpendicular to the workpiece surface, the centre of the tool is stationary in relation to the workpiece surface. This can be seen in Figure 21.

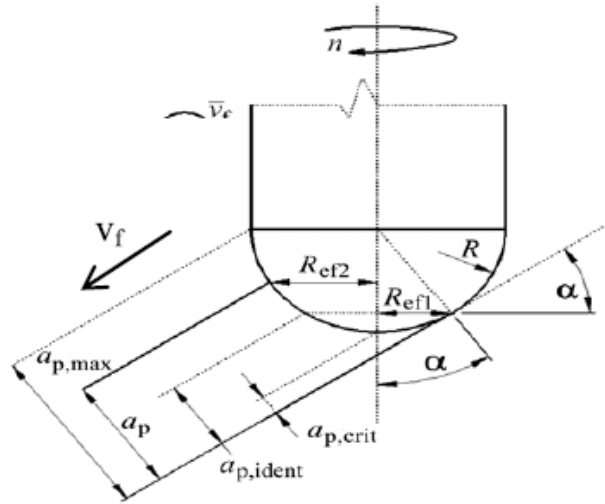


Figure 20 - Downward ramping [31].

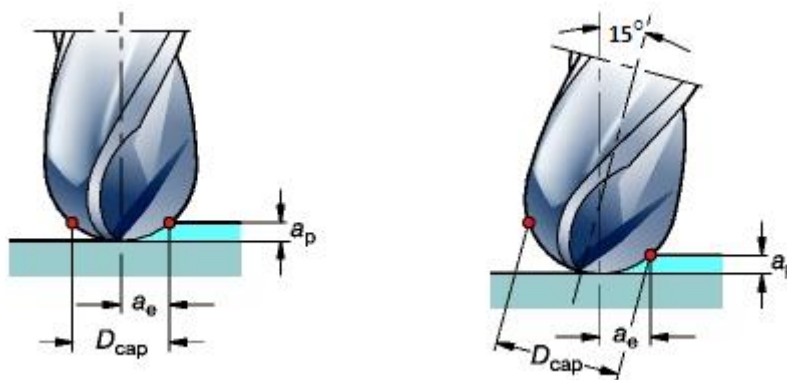


Figure 21 - Non-tilted versus tilted cutter [32].

A fixture was developed and 3D printed to ensure that the worn part of the cutting tool was perpendicular to the microscope during the measurement. The optical 3D measurement results in a 3D image of the worn tool and an example can be seen in Figure 22. To measure the flank wear the 3D image is transformed to a 2D image, see Figure 23. From the 2D image the profile of the cutting edge can be plotted and the wear can be measured, which can be seen in Figure 24. The curve of the worn tool profile can be compared to the one of a new tool in Figure 25.

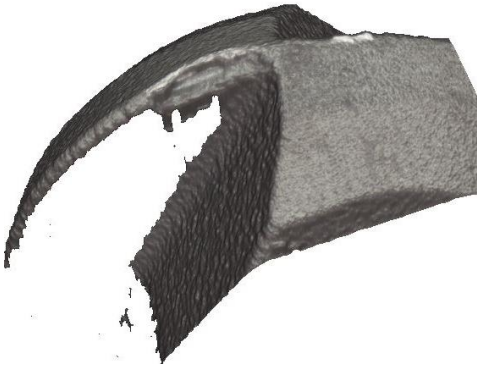


Figure 22 - 3D image of worn Zecha ball nose end mill

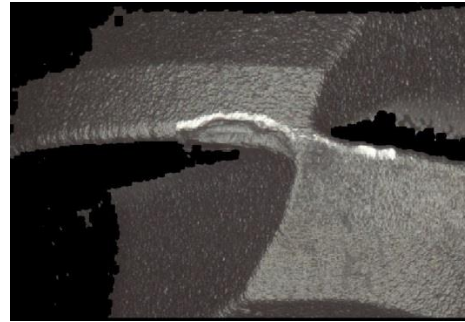


Figure 23 – 2D image of worn Zecha ball nose end mill

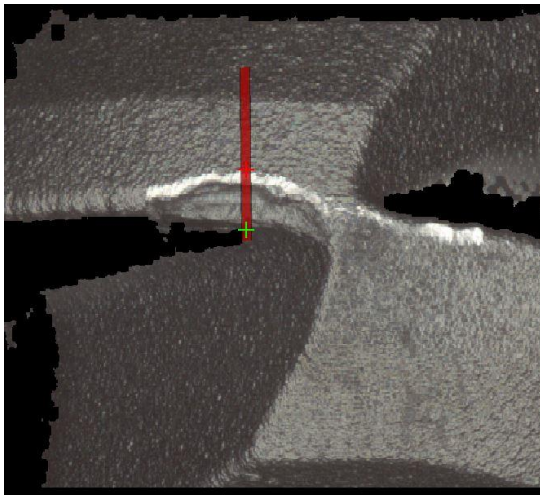


Figure 24 – 2D image of worn Zecha ball nose end mill with plotted profile

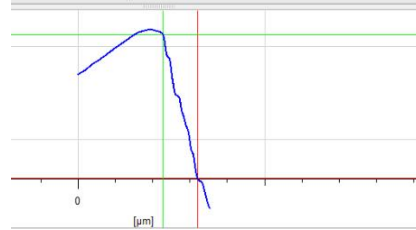
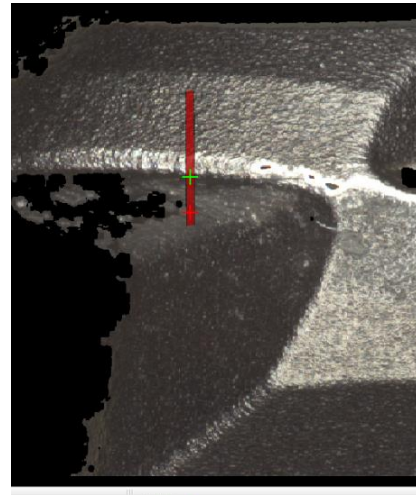


Figure 25 – 2D image of a new ball nose end mill with plotted profile.

To compare the different cutting tools the length a tool travels in the workpiece was calculated. A sketch of the length is found in Figure 26 and the length is calculated with the equations (6) – (8).

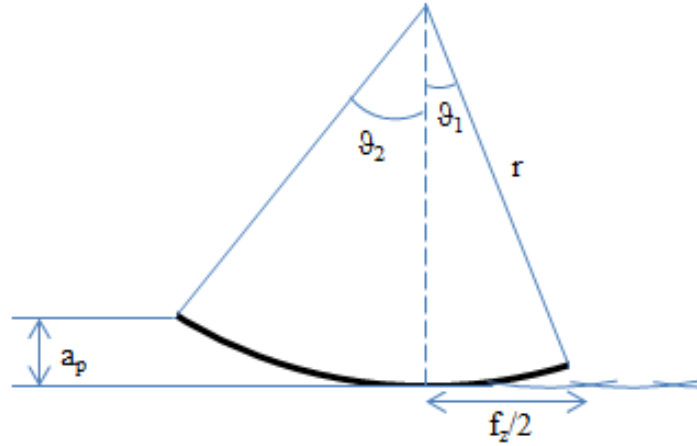


Figure 26 - Cutter travelled distance.

$$L = \vartheta * R = (\vartheta_1 + \vartheta_2) * R \quad (6)$$

$$\vartheta_1 = \sin^{-1} \frac{f_z}{2 * R} \quad (7)$$

$$\vartheta_2 = \cos^{-1} \frac{r - a_p}{R} \quad (8)$$

Further analysing included surface roughness tests using a 3D optical microscope from Veeco. Also the surface contents and surface integrity was studied using a scanning electron microscope (SEM). The workpieces were also cut and moulded into resin to study the cross-section of the surface using SEM. The tests are designed to study the effect of binder content and also what effect different tool materials have on tool wear and surface integrity.

3.2 Expectations

Based on the theory in the previous chapter, a couple of predictions can be stated before the experiments are performed.

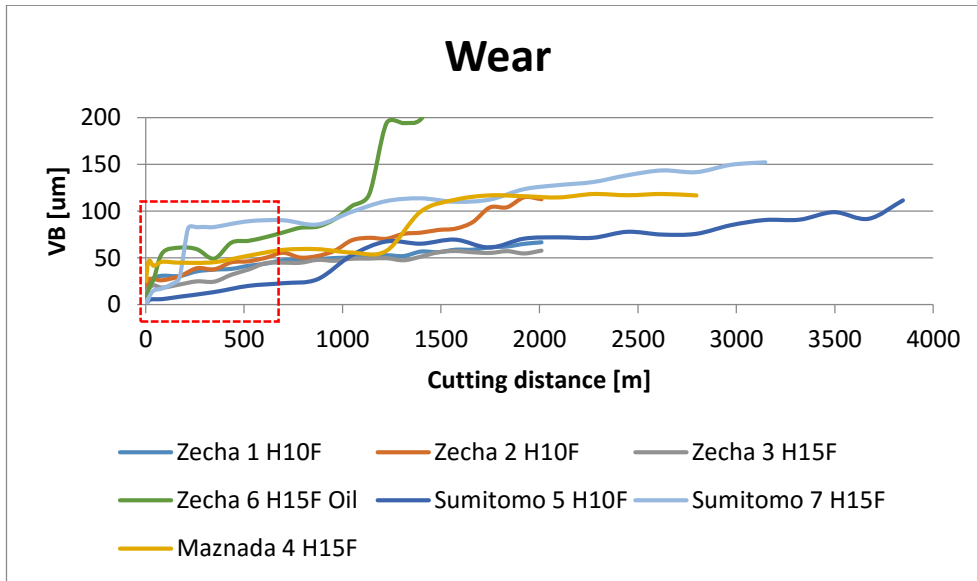
Tool wear: The tool wear is expected to differ for the different tools, also the two workpiece materials should lead to unequal tool wear. For all tools the wear should be more rapid in the tool material H10F compared to H15F. Since H10F contains a larger content of tungsten carbide, the material is harder and more abrasive. Regarding the different tools, the NPDB tool is the hardest tool and is expected to be the most wear resistant.

Surface integrity: Since the cutting data is selected in order to achieve ductile cutting, the cut surface is expected to have a fine surface roughness. The NPDB tool has a sharper cutting edge and should be able to provide a finer surface roughness compared to the other tools.

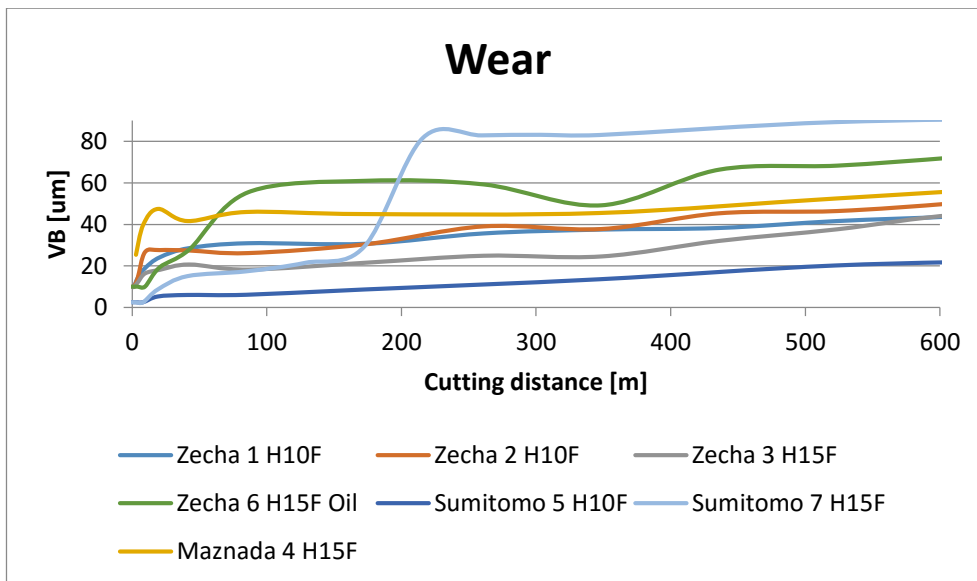
3.3 Experimental results and discussion

The wear measurements are presented as graphs below in Graph 1 to Graph 4. In Graph 1 all the collected wear data are plotted and Graph 2 focuses on the first 600 meters of cutting distance highlighted in Graph 1. Graph 3 and Graph 4 separate the tools by their number of flutes. The surface roughness measurements are presented in Graph 5 and Graph 6. SEM images of the workpiece surface and the tool wear of corresponding position is presented for Zecha 6 H15F in Figure 30 to Figure 35 and Sumitomo 5 H10F in Figure 36 to Figure 41. Last in the chapter 3D images of the workpiece surface is presented for Sumitomo 5 H10F in Figure 42 to Figure 44. The EDS results are presented in Table 4.

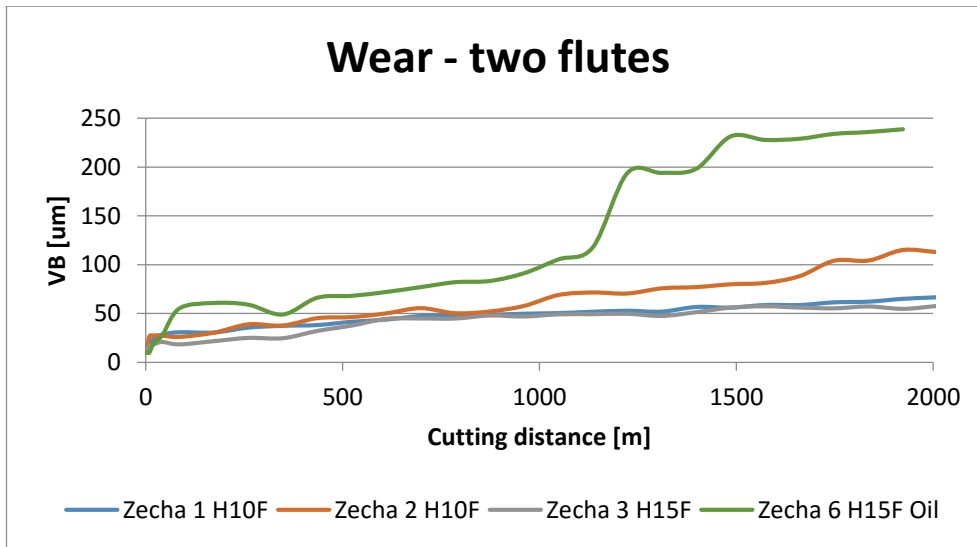
3.3.1 Results and discussion regarding wear



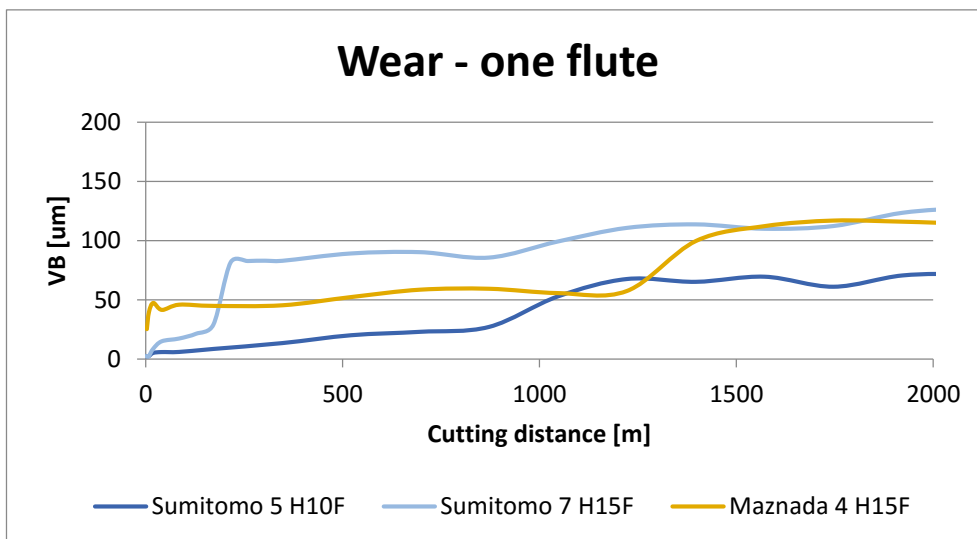
Graph 1 - Tool wear plotted against cutting distance for all used tools.



Graph 2 - Tool wear plotted against cutting distance for all used tools with focus on the first 600 meters, highlighted in Graph 1.



Graph 3 - Tool wear plotted against cutting distance for the tools with two flutes.



Graph 4 - Tool wear plotted against cutting distance for the tools with one flute.

The main issue for this project was to investigate how the binder content affects the machinability for cemented carbide. In Graph 1 to Graph 4 the wear results are displayed and there are two pairs of tools that are important to compare in order to see the influence of the binder. First off it can be seen that for the tests Zecha 1 H10F and Zecha 3 H15F the wear was almost identical, which was not predicted. It can also be seen that for the test Zecha 2 H10F, which should be identical to Zecha 1 H10F, the wear curves are similar in the beginning, but the wear increases for Zecha 2 H10F in the end. The reason for the incensement was failure to fasten the workpiece in the vice, which caused the workpiece to tilt during machining and increasing the cutting depth.

Secondly the tests Sumitomo 5 H10F and Sumitomo 7 H15F are important to investigate. In Graph 4 it can be seen that the wear curves behave almost the same, except a sudden escalation after about 170 meters for Sumitomo 7 H15F. In order to explain the escalation in the wear curve, the images from the Alicona measurement are studied. In the images for Sumitomo 7 H15F it can be seen that a crack in the tool was developed, which resulted in part of the tool was chipped off, see Figure 27 to Figure 29. The tool in test Sumitomo 5 H10F did not develop any crack and the wear was much more uniform. The differences between the two Sumitomo tools are likely to be a result of circumstance, for example a slight difference in tool strength after manufacturing. The overall results indicate that the binder content difference between 10% and 15% cobalt do not affect the wear significantly.



Figure 27 – Initial crack Zecha 7 H15F.



Figure 28 – Crack Zecha 7 H15F.

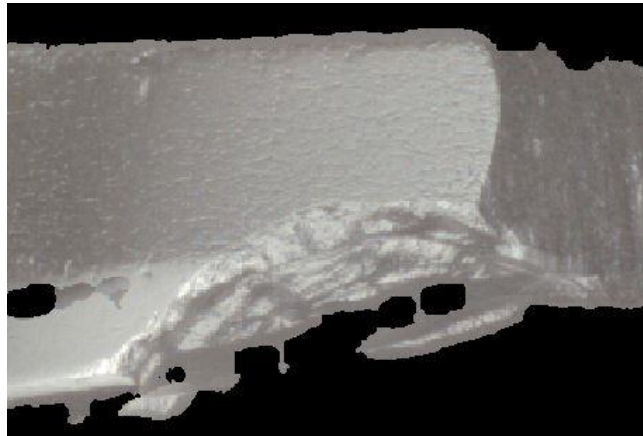
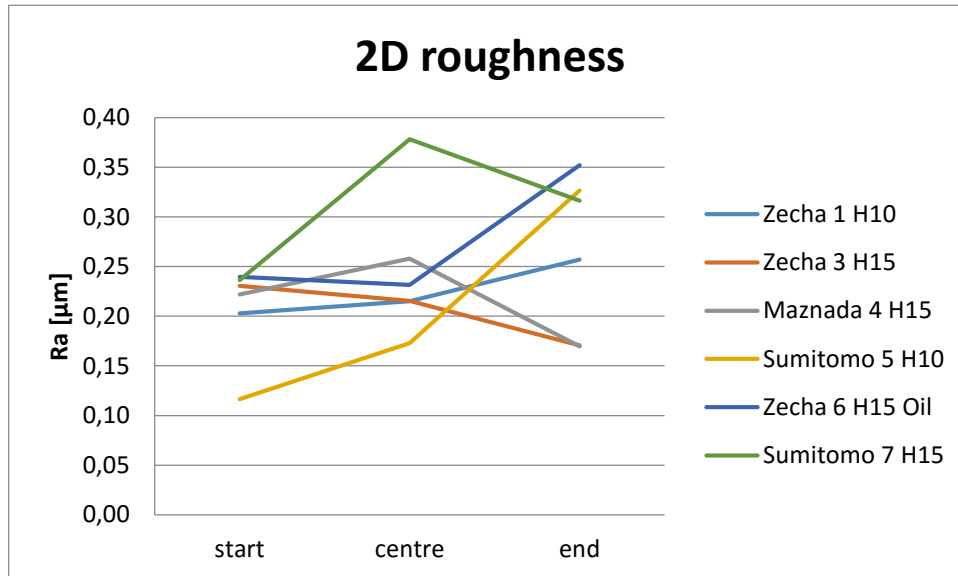


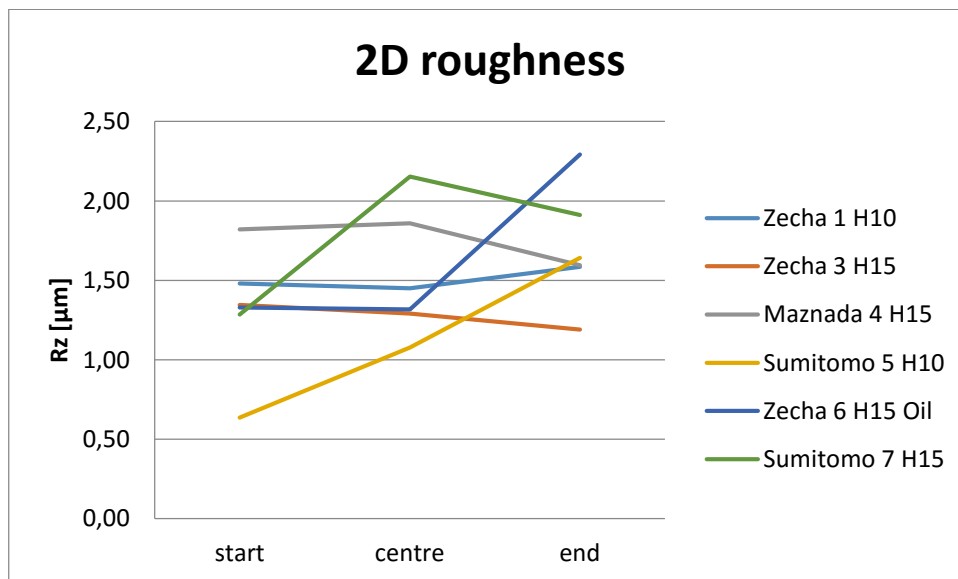
Figure 29 – Totally cracked Zecha 7 H15F.

The tool maker Sumitomo recommended that the NPDB tool was cooled with oil mist while Zecha did not recommend a coolant. The sixth test with Zecha was cut with oil mist as coolant, in order to see if the coolant affected the wear. It can be seen in Graph 3 that the wear increased rapidly when applying oil as coolant for Zecha. When investigating the Alicona images of the tool wear, it was seen that the coating was totally peeled off, seen in Figure 35 below. A possible explanation could be that the oil penetrated the area between the coating and the tool. The pressure created during each cutting initiation might then result in the coating being peeled off. This is of course only one possible explanation.

3.3.2 Results and discussion regarding surface roughness



Graph 5 – R_a measured at three positions.



Graph 6 - R_z measured at three positions.

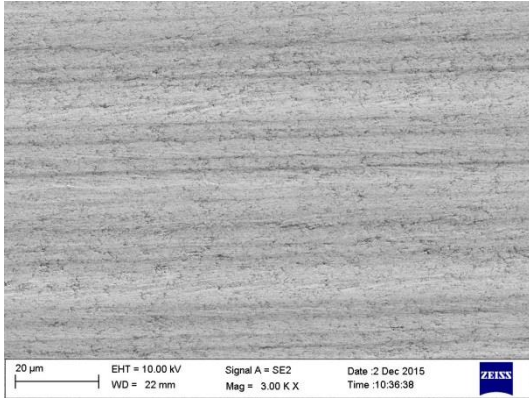


Figure 30 – SEM image of Zecha 6 H15F Oil start position.

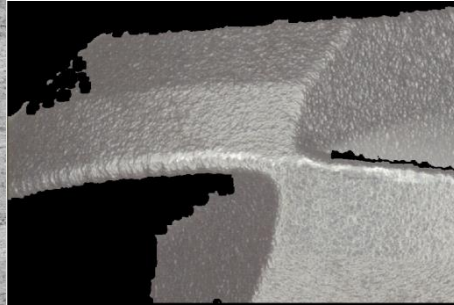


Figure 31 – Tool wear of Zecha 6 H15F Oil start position.

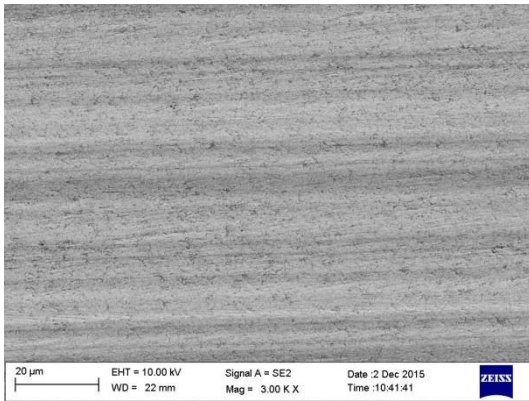


Figure 32 – SEM image of Zecha 6 H15F Oil centre position.

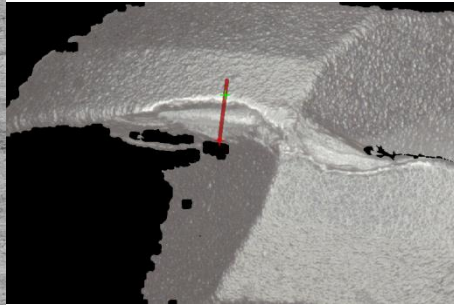


Figure 33 – Tool wear of Zecha 6 H15F Oil centre position.

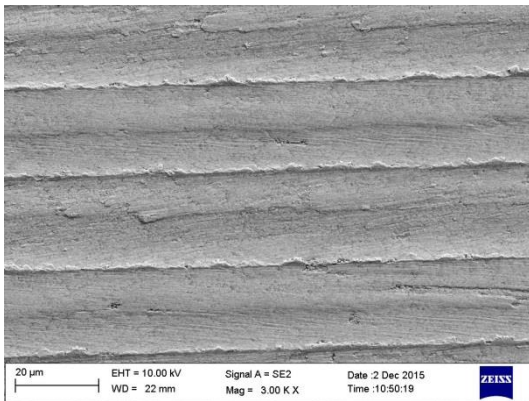


Figure 34 – SEM image of Zecha 6 H15F Oil end position.

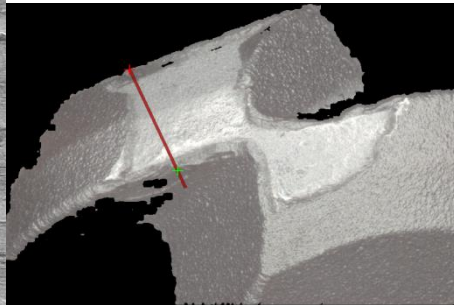


Figure 35 – Tool wear of Zecha 6 H15F Oil end position.

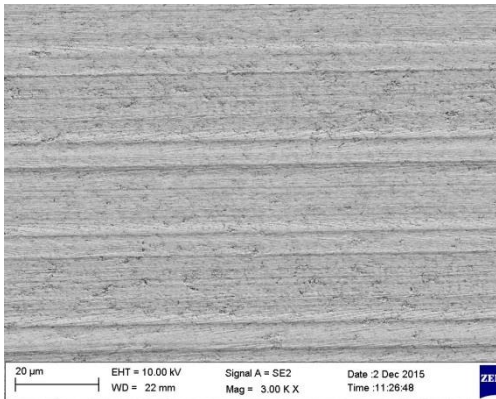


Figure 36 – SEM image of Sumitomo 5 H10F start position.

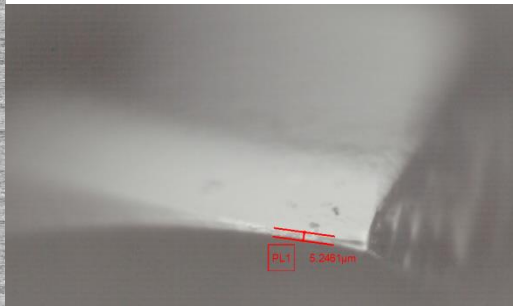


Figure 37 – Tool wear of Sumitomo 5 H10F start position.

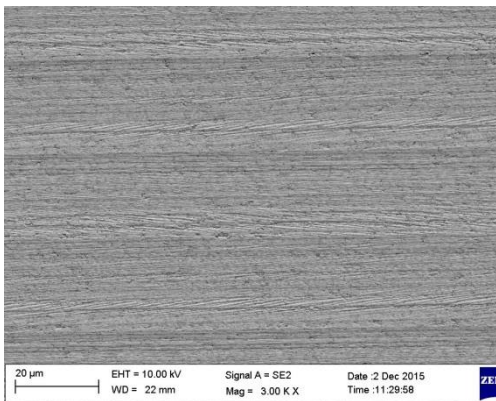


Figure 38 – SEM image of Sumitomo 5 H10F centre position.

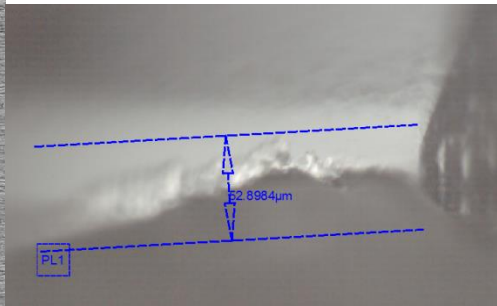


Figure 39 – Tool wear of Sumitomo 5 H10F centre position.

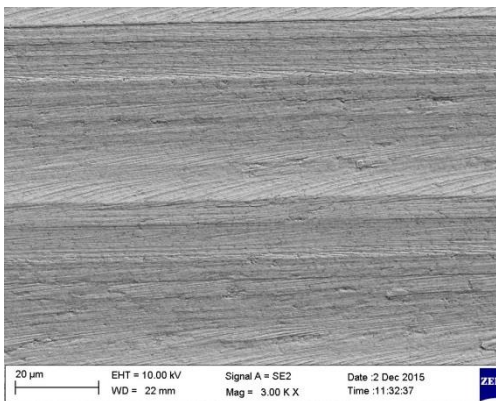


Figure 40 – SEM image of Sumitomo 5 H10F end position.

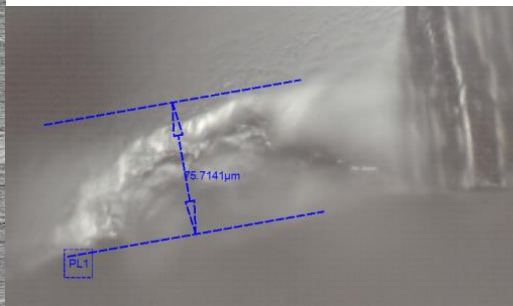


Figure 41 – Tool wear of Sumitomo 5 H10F end position.

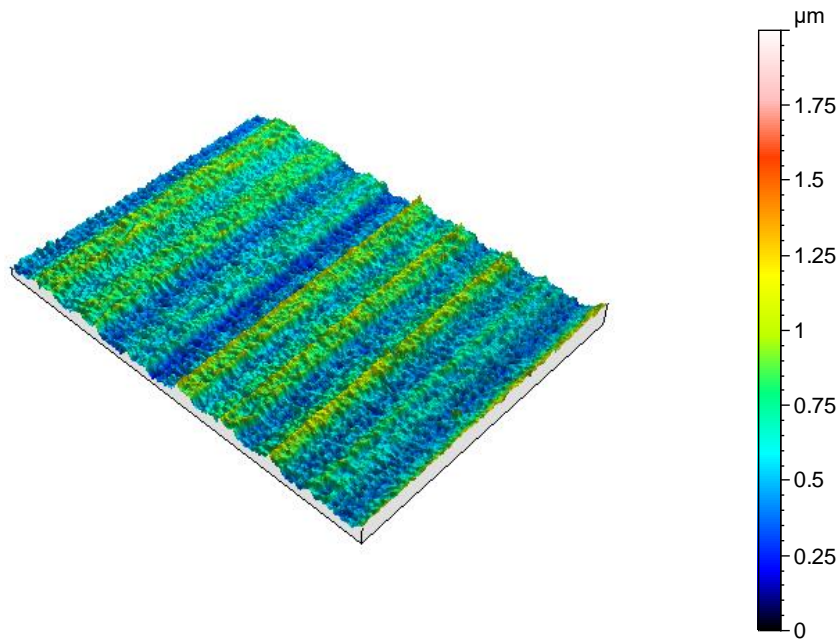


Figure 42 -3D surface Sumitomo 5 H10F start position.

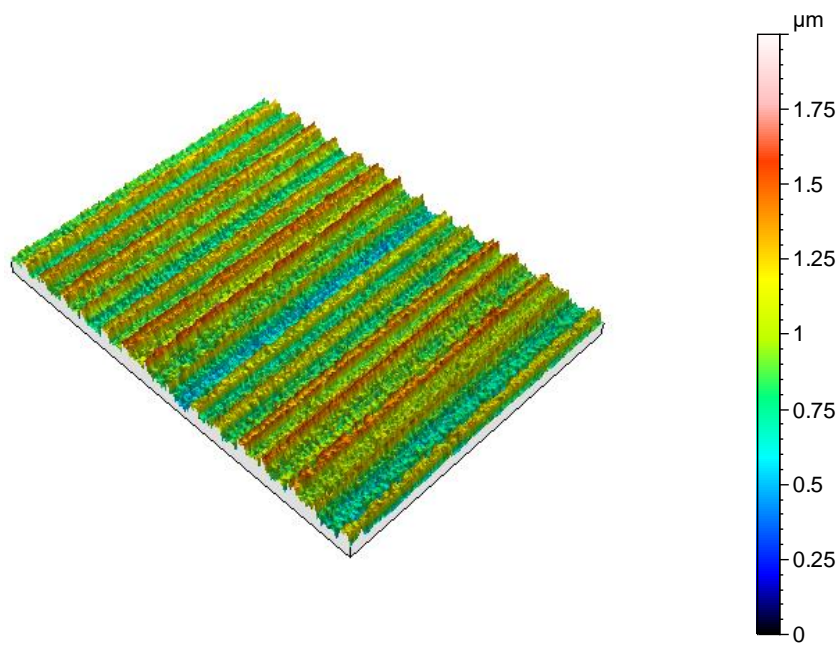


Figure 43 – 3D surface Sumitomo 5 H10F centre position.

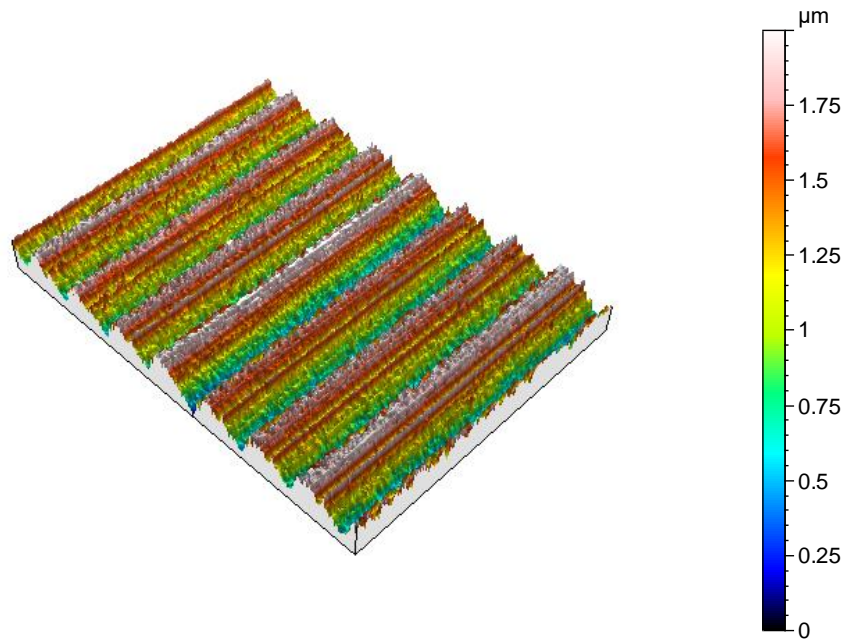


Figure 44 - 3D surface Sumitomo 5 H10F end position.

When studying Graph 5 and Graph 6 it is apparent that all the tools cut surfaces with similar roughness. The Sumitomo tool has the sharpest tool edge radius at 5 μm and the Zecha tool an edge radius of 20 μm , which theoretically meant that the Sumitomo tool could produce a smoother surface. As predicted it can be seen that the Sumitomo test 5 in H10F created the finest surface, which is in line with theory. The rougher surface in test 7 Sumitomo H15F could be explained by the fact that the tool cracked. The observed position on the workpiece might be after the cracking of the tool edge, which would lead to a rougher surface. The surfaces that were cut are positioned in the interval of 0.12 μm to 0.38 μm in R_a .

It was mentioned earlier that the coating of the Zecha tool was peeled off at the end of the sixth test, which resulted in the cut surface seen in Figure 34 with lots of side flow. In order to explain the appearance of the cut surface, it is important to notice that the thickness of the coating of the tool was 15 μm and the cutting depth was 20 μm . After the moment that the coating was peeled off, the real cutting depth was 5 μm which was not enough to shear a chip. The phenomenon is seen in equation (3), if the cutting depth decreases the undeformed chip thickness decreases which affects the relationship between the undeformed chip thickness and the tool edge radius. When the undeformed chip thickness became too small, no cutting was performed. Instead the tool plowed the surface which created the surface seen in Figure 34.

The surface created by the Zecha tool can be compared to the results from the Sumitomo tool shown in Figure 36 to Figure 41. Both tools created a cut surface in the beginning and at the center, but the Sumitomo tool cut the workpiece until the end. Because the Sumitomo tool is solid, each time a part of the tool was chipped off a new cutting edge was created until the tool was completely worn out. When the tool geometry changes during the wear process the cut surface geometry changes. This can be seen in Figure 42 to Figure 44. When the tool gets worn out it creates a rougher surface on the workpiece, which is in line with available theory.

The fourth test with the Maznada tool was performed as a bonus test. The tool was already available in Gimo and the test was performed in order to collect extra data. It can be seen that the wear was in the same range as for the other tools, see Graph 2. It was also able to produce a similar surface roughness as the other tools, only the Sumitomo tool was better. Since it was a cemented carbide tool with a diamond coating, the cost was in the same price range as the Zecha tool. Because the tool was only tested in one material, no conclusions regarding the binder content could be drawn. But the results indicate that the cheaper tool might be a viable choice if the surface quality is not the main factor.

3.3.3 Results discussion regarding surface content

Table 4 – EDS analysis of the surface.

	Position	Tungsten [%]	Cobalt [%]
Zecha 1 H10F	Bulk material	87.6	12.4
	Start	86.8	13.2
	Centre	87.2	12.8
	End	87.7	12.3
Zecha 3 H15F	Bulk material	81.3	18.7
	Start	80.2	19.8
	Centre	82.0	18.0
	End	82.6	17.4
Sumitomo 5 H10F	Bulk material	87.6	12.4
	Start	90.5	9.5
	Centre	91.1	8.9
	End	91.9	8.1
Sumitomo 7 H15F	Bulk material	81.3	18.7
	Start	86.4	13.6
	Centre	85.1	14.9
	End	83.7	16.3

The hydrostatic pressure that is created when cutting a brittle material in a ductile way might help explaining the EDS result from Table 4, where it is seen that the tungsten carbide content at the surface increases as the tool gets more worn out. The pressure deforms the tungsten carbide, flattening it out at the surface. When the tungsten carbide is flattened, the cobalt is pressed down deeper into the workpiece. As the tool gets more worn out, the hydrostatic pressure increases and more cobalt is pressed down into the workpiece.

4 Conclusions

What surface quality can be obtained?

The surface roughness obtained in the experiments range from 0.12 μm to 0.38 μm in R_a . Since the experiment did not focus on obtaining the optimal surface roughness it could be possible to select different cutting data in order to optimize the surface roughness. If the tool is too worn out, no cutting takes place. Instead the surface is plowed by the tool and result in side flow.

What does the machined cemented carbide surface consist of, after machining?

The machined surface consists of tungsten carbide and cobalt, the tungsten carbide content increases if the hydrostatic load increases. This is explained by the tungsten carbide being flattened and the cobalt pressed into the workpiece as a result of the deformation.

Is there an economically preferable binder content?

The tests showed that a difference in 5% binder, from 10% to 15%, did not increase the wear propagation speed. The selection between 10% and 15% binder does not affect the economical side of the cutting process.

How is the machinability of cemented carbide affected by the binder content in terms of tool life, surface quality and an economical aspect, when machined with coated cemented carbide or diamond tools?

The machinability is not affected by a change in binder content from 10% to 15% cobalt. Tool life and surface quality are more dependent on tool shape and tool material. Since the tool life was similar for the different tools it is more economical to use the cheaper cemented carbide tool compared to the NPDB tool. Although since the surface quality obtained with the NPDB tools is finer, the tool is better if the surface quality is important. An advice for future applications could be to use the cemented carbide tool for rough machining and the NPDB tool for finishing.

5 Future work

Future work could include testing of other tool materials. For example materials based on boron nitride, that belong to the second hardest material group next to diamonds. The one with cubic crystal structure is the hardest of this group and has a high level of heat and chemical resistance. cBN tools are commercially available today and are used in cutting operations of hardened steel, grey cast iron and powder metals. Traditionally cBN is produced by mixing a powder of fine cBN grains with a binder or catalyst and sinter it at temperatures of 1300 - 1500 °C at pressures of 4 - 6 GPa [7]. Recent research has resulted in nbcBN that is not mixed with any binder or catalyst, hence the name binderless.

nbcBN is produced by transforming hexagonal boron nitride (hBN) into cubic boron nitride (cBN) under high pressures of 5 - 8 GPa and temperatures higher than 1500 °C [33]. The process result in a super hard disk of nbcBN that can be ground into the desired tool geometry with use of a diamond coated disc. Since the grains are fine and no binder is present, the tool edge can be as sharp as the ones of a single-crystal diamond tool, but since cBN is composed by numerous boundaries between fine particles it is more durable than single-crystal diamond. Grain boundaries are found in polycrystalline materials and are defects in the crystal structure. The defects restrain dislocations in the material. Thus in a material with few or no grain boundaries, slip that occur when the material is sheared meet less resistance compared to a material with many boundaries. This phenomenon can clearly be seen in work hardening of for example steel, where the grains are deformed to decrease in size which creates more grain boundaries and thus a tougher material. This mechanism also applies to cemented carbide and polycrystalline diamond. The cBN tools can be re-polished and therefore re-used which leads to a more economical production [34].

Theoretically nbcBN as tool material for cutting cemented carbide is an interesting choice and future testing is recommended in order to explore its potential.

REFERENCES

- [1] Sandvik Group, "Sandvik's business areas," Sandvik Group, [Online]. Available: <http://www.sandvik.com/en/about-us/our-company/business-areas/>. [Accessed 16 September 2015].
- [2] Sandvik Coromant, "Sandvik Coromant in brief," Sandvik Coromant, [Online]. Available: http://www.sandvik.coromant.com/en-gb/aboutus/sandvik_coromant_in_brief/Pages/default.aspx. [Accessed 16 September 2015].
- [3] Sandvik Coromant, "Our history," Sandvik Coromant, [Online]. Available: http://www.sandvik.coromant.com/en-gb/aboutus/our_history/pages/default.aspx. [Använd 17 September 2015].
- [4] Sandvik Coromant, "Products," Sandvik Coromant, [Online]. Available: <http://www.sandvik.coromant.com/en-gb/products>. [Använd 17 September 2015].
- [5] Sandvik Coromant, "CoroMill Plura," Sandvik Coromant, [Online]. Available: http://www.sandvik.coromant.com/en-gb/products/coromill_plura/Pages/Product-details.aspx. [Använd 07 12 2015].
- [6] Sandvik Coromant, "RA216-16EH16," Sandvik Coromant, [Online]. Available: <http://www.sandvik.coromant.com/en-gb/products/pages/productdetails.aspx?c=ra216-16eh16&m=6550054>. [Använd 07 12 2015].
- [7] J.-E. Ståhl, *METAL CUTTING - Theories and Models*, Lund: Jan-Eric Ståhl, 2012.
- [8] K. Liu, X. Li och M. Rahman, "CBN tool wear in ductile cutting of tungsten carbide," i *14th International Conference on Wear of Materials*, Washington, 2003.
- [9] G. Zurek, "Understanding Micro-Milling Machine Technology," *Production Machining*, 8 December 2008. [Online]. Available: <http://www.productionmachining.com/articles/understanding-micro-milling-machine-technology>. [Använd 5 October 2015].
- [10] M. J. Jackson, "Theory of Micromachining," i *Micro and Nanomanufacturing*, West Lafayette, Springer Science+Business Media, LLC, 2007, pp. 195-196.
- [11] A. Sharman, R. C. Dewes och D. K. Aspinwall, "Tool life when high speed ball nose end milling Inconel 718," *Journal of Materials Processing Technology*, vol. 118, nr 1-3, p. 29, 2001.
- [12] F. Klocke, *Manufacturing Processes 1*, Berlin: Springer, 2011.
- [13] S. Debnah, M. M. Reddy och Q. S. Yi, "Environmental friendly cutting fluids and cooling techniques in machining: a review," *Journal of Cleaner Production*, vol. 83, pp. 33-47, 2014.
- [14] Sandvik Coromant, "Coated cemented carbide," Sandvik Coromant, [Online]. Available: http://www.sandvik.coromant.com/en-gb/knowledge/materials/cutting_tool_materials/coated_cemented_carbide. [Använd 30 September 2015].

-
- [15] Sandvik Hard Materials, "Nano, ultrafine and submicron grades," Sandvik Hard Materials, 2008. [Online]. Available: http://www.allaboutcementedcarbide.com/02_01.html. [Använd 30 September 2015].
- [16] Sandvik, "Sandvik H10F," Sandvik, August 2001. [Online]. Available: [http://www2.sandvik.com/sandvik/0130/Internet/se03460.nsf/Alldocs/Pdfs*2A913*5F916/\\$file/H2062H10F.pdf](http://www2.sandvik.com/sandvik/0130/Internet/se03460.nsf/Alldocs/Pdfs*2A913*5F916/$file/H2062H10F.pdf). [Accessed 22 September 2015].
- [17] Sandvik, "Sandvik H15F," Sandvik, April 2002. [Online]. Available: [http://www2.sandvik.com/SANDVIK/0130/Internet/SE03460.NSF/Index/4f1919ae98ff8704c12571da002ec484/\\$FILE/H15F.pdf](http://www2.sandvik.com/SANDVIK/0130/Internet/SE03460.NSF/Index/4f1919ae98ff8704c12571da002ec484/$FILE/H15F.pdf). [Accessed 22 September 2015].
- [18] H. Shimada, K. Yano and Y. Kanada, "Sumidia Binderless Ball-Nose Endmills "NPDB" for Direct Milling of Cemented Carbide," *SEI TECHNICAL REVIEW*, pp. 86-90, October 2014.
- [19] Sumitomo Electric, "Sales of NPDB Mold Finish Master SUMIDIA binderless ballnose endmills launched," Sumitomo Electric, 14 January 2015. [Online]. Available: http://global-sei.com/company/press/2015/01/prs14109_s.html. [Använd 30 September 2015].
- [20] ZECHA, "NEW! MARLIN - Highly hart cutting tools for the machining of solid carbide," [Online]. Available: <http://www.zecha.de/de/340-neu-marlin>. [Använd 07 12 2015].
- [21] Sumitomo Electric Industries, Ltd., "Mold Finish Master NPDB - Direct milling on cemented carbide materials," 2015. [Online]. Available: <http://www.sumitool.com/en/products/cutting-tools/endmills/npdb.html>. [Använd 07 12 2015].
- [22] Sandvik Coromant, "Polycrystalline diamond," Sandvik Coromant, [Online]. Available: http://www.sandvik.coromant.com/en-gb/knowledge/materials/cutting_tool_materials/polycrystalline_diamond/Pages/default.aspx. [Använd 30 September 2015].
- [23] Sandvik Coromant, "Measuring Surfaces," Sandvik Coromant, [Online]. Available: http://www.sandvik.coromant.com/en-gb/knowledge/materials/measuring_surfaces. [Accessed 25 September 2015].
- [24] Metal Improvement Company, "Concept of Stress Intensity Superposition," Curtiss-Wright Corporation, 2010. [Online]. Available: http://www.metalimprovement.com/laserpeening_residualstress.php. [Använd 5 11 2015].
- [25] K. Liu, X. Li och S. Liang, "The mechanism of ductile chip formation in cutting of brittle materials," *The International Journal of Advanced Manufacturing Technology*, vol. 33, nr 9, pp. 875-884, 2007.
- [26] P. Bridgman, "Effects of Very High Pressures on Glass," *Journal of Applied Physics*, vol. 24, nr 4, pp. 405-413, 1953.
- [27] K. Woon, M. Rahman, F. Fang, K. Neo och K. Liu, "Investigations of tool edge radius effect in micromachining: A FEM simulation approach," *journal of materials processing technology*, vol. 195, nr 1-3, pp. 204-211, 2008.
- [28] K. Liu och X. Li, "Ductile cutting of tungsten carbide," *Journal of Materials Processing Technology*, vol. 113, nr 1-3, pp. 348-354, 2001.
- [29] M. Field och K. JF, "Review of surface integrity of machined components," *CIRP Ann*, vol. 20, nr 2, pp. 153-63, 1971.
-

-
- [30] F. M, K. JF och C. J, "Review of measuring methods for surface integrity," *CIRP Ann*, vol. 21, nr 2, pp. 219-38, 1972.
- [31] T. Vopát, J. Peterka, M. Kováč och I. Buranský, "The Wear Measurement Process of Ball Nose end Mill in the Copy Milling Operations," *Procedia Engineering*, vol. 69, pp. 1038-1047, 2014.
- [32] Sandvik Coromant, "Application checklist," Sandvik Coromant, [Online]. Available: http://www.sandvik.coromant.com/en-gb/knowledge/milling/application_overview/profile_milling/application_checklist. [Använd 17 11 2015].
- [33] T. Taniguci, M. Akaishi och S. Yamaoka, "Sintering of cubic boron nitride without additive at 7.7 GPa and above 2000 °C," i *Journal of Materials Research*, 1999, pp. 162-169.
- [34] K. Fujisaki, H. Yokota, N. Furushiro, Y. Yamagata, T. Taniguchi, R. Himeno, A. Makinouchi och T. Higucho, "Development of ultra-fine-grain binderless cBN tool for precision cutting of ferrous materials," i *Journal of Materials Processing Technology*, ELSEVIER, 2009, p. August.